Available online at www.sciencedirect.com
ScienceDirect
Advances in Space Research 47 (2011) 1674–1680
ADVANCES IN SPACE RESEARCH (a COSPAR publication)
www.elsevier.com/locate/asr

First evidence of anisotropy of GPS phase slips caused by the mid-latitude field-aligned ionospheric irregularities

E.L. Afraimovich [a], A.B. Ishin [a], M.V. Tinin [b], Yu.V. Yasyukevich [a,b,*], S.G. Jin [c]

[a] Institute of Solar-Terrestrial Physics SB RAS, 126a, Lermontov street, Irkutsk 664033, P.O. Box 291, Russian Federation
[b] Irkutsk State University, 20 Gagarin Blvd, Irkutsk 664003, Russian Federation
[c] Shanghai Astronomical Observatory, Chinese Academy of Sciences, Shanghai 200030, China

Received 8 February 2010; received in revised form 11 December 2010; accepted 13 January 2011
Available online 23 January 2011

Abstract

The mid-latitude field-aligned irregularity (FAI) along the magnetic field line is a common phenomenon in the ionosphere. However, few data reveal the field-aligned ionospheric irregularities. They are insufficient to identify FAIs effects so far, particularly effect on global positioning system (GPS) signals. In this paper, the mid-latitude FAIs by line-of-sight angular scanning relative to the local magnetic field vector are investigated using the denser GPS network observations in Japan. It has been the first found that total GPS L2 phase slips over Japan, during the recovery phase of the 12 Feb 2000 geomagnetic storm were caused by GPS signal scattering on FAIs both for the lines-of-sight aligned to the magnetic field line (the field of aligned scattering, FALS) and across the magnetic field line (the field of across scattering, FACS). The FALS results are also in a good agreement with the data of the magnetic field orientation control of GPS occultation observations of equatorial scintillation during thorough low earth orbit (LEO) satellites measurements, e.g. Challenging Minisatellite Payload (CHAMP) and Satellite de Aplicaciones Cientificas-C (SAC-C). The role of large-angle scattering almost along the normal to the magnetic field line in GPS scintillation is determined by attenuation of the irregularity anisotropy factor as compared with the other factors.

Keywords: GPS phase slip; Field-aligned irregularity (FAI); Ionosphere; Magnetic field

1. Introduction

Strong scintillations of amplitude and phase of transionospheric radio signals occur due to signal scattering on intensive small scale irregularities (Yeh and Liu, 1982). The scale of such irregularities is by the order of the Fresnel first zone radius, 150–300 m for $f_1 = 1575.25$ MHz, $f_2 = 1227.2$ MHz GPS frequencies. The scintillation has an adverse effect on GPS signals and causes a GPS receiver to lose locking the signal in some extreme cases. The expansion of the auroral oval equatorward is known to be followed by an increase in slips of satellite signal tracking and GPS positioning deterioration in the mid-latitude region (Afraimovich et al., 2002, 2003, 2009).

Ionospheric irregularities and steep gradients often occur at high-latitude ionosphere considerably disturbed due to auroral substorms. Over recent years, extensive studies of mid-latitude phase fluctuations and GPS phase slips under geomagnetic disturbance condition have been made (Skone, 2001; Conker et al., 2003; Ledvina et al., 2002, 2004; Ledvina and Makela, 2005; Afraimovich et al., 2002, 2003, 2009; Cerruti et al., 2006; Astafyeva et al., 2008; Meggs et al., 2006; Jin et al., 2008). Though the mid-latitudes are considered comparatively quiet, strong plasma density disturbances are often observed here. For example, this can be related to the auroral oval expanding especially during geomagnetic storms. Existence of the ionization anomaly at low-latitudes, along with the well-known effect of the equatorial plasma bubble

* Corresponding author. Tel.: +7 3952 564554; fax: +7 3952 511675.
E-mail addresses: afra@iszf.irk.ru (E.L. Afraimovich), ishin@iszf.irk.ru (A.B. Ishin), mtinin@api.isu.ru (M.V. Tinin), yasukevich@iszf.irk.ru (Yu.V. Yasyukevich), sgjin@shao.ac.cn (S.G. Jin).

0273-1177/$36.00 © 2011 COSPAR. Published by Elsevier Ltd. All rights reserved.
doi:10.1016/j.asr.2011.01.015

formation during evening hours, also increases the possibility for transionospheric signal to fade in this region. Plasma bubbles are associated with equatorial spread F (ESF) processes. A plasma bubble evolves along the Earth's magnetic field line. It is stretched in the meridian direction, but narrow in the zonal one. A plasma bubble has a finite height, and its poleward limit is determined by its equatorial height. Equatorial bubbles are not often observed at mid-latitudes. In sparse cases the ESF density depletions can reach high altitudes and extend to the equatorial anomaly latitudes. For example, satellite measurements showed that the ESF plasma depletions can reach apex altitude of 2000–6000 km (Burke et al., 1979; Ma and Marayama, 2006; Huang et al., 2007).

Although the ESF plasma bubble is a common phenomenon and has been studied for years, precise observational data on ionospheric scintillations and loss of locking GPS signals at mid-latitude are still limited. Post-sunset bubbles, revealed by a loss of L2 signal lock, were observed at mid-latitudes (~30°–34°N, ~130°–134°E) during the main phase of the 12 Feb 2000 storm (Ma and Marayama, 2006). The bubble had unusually large latitudinal extension reaching 36.5°N (31.5°N magnetic latitude), which corresponds to the apex height of ~2500 km. However, there are no data on space geometry of field-aligned irregularities in the past time. For example, Ma and Marayama (2006) have identified their observations as bubbles using only the following criteria like the occurrence time (post sunset), the presence of phase slips, and total electron content (TEC) as well as local density depletion at the Defense Meteorological Satellite Program (DMSP). However, the above criteria are insufficient to identify bubbles. One should obtain some direct evidence of the structure oblongness (i.e. field-aligned irregularities, FAI) along the magnetic field line. In this paper, it aims to present the method of GPS to detect the mid-latitude FAIs by using loss of L2 signal lock, and to estimate their characteristics with example of the 12 Feb 2000 unusual event.

2. Mid-latitude field-aligned disturbances

The basic idea of our method is that if irregularity is extended lengthways the magnetic fields the effects on radio signal parameters significantly depends on orientation of a line-of-sight against the magnetic field. So there is the angular dependence of radio signal parameters distortions. If corresponding distinctions at different angles are found, it is possible to make conclusion about spatial orientation of registered large-scale irregularity. GPS signal amplitude scintillations connected with bubbles can cause the phase slip. So for a dense GPS network phase slips can be used as an indicator of the irregularity orientation.

Although Ma and Marayama (2006) analyzed loss of L2 signal lock for each selected satellite, but just used only 300 homogeneously selected GEONET GPS stations. While all the GEONET GPS data (~1000) are used to analyze in our study. These data are available in the standard RINEX format with 30 s sampling intervals. The L2 slips from RINEX files (Gurtner, 1993) are detected using the standard GPS technology. Also, we determined the azimuth α_S and the line-of-sight (LOS) elevation θ_S between a GPS site and a satellite. Lower signal/noise ratio at L2 is primarily determined by the fact that the GPS satellite L2 transmitter power is 6 dB less than the fundamental frequency f1 with the C/A code (ICD-200c). Similar correlation of the L1 effective radiated power (30 watt) and L2 (21 watt) signals are also typical of the Russian GLONASS system (Perov and Kharisov, 2005). Phase slips at L2 may also be caused by a higher signal/noise ratio for L2 when commercial non-coded receivers are used. Such receivers have no access to the military $\ll$ Y $\gg$ code, and they are using the non-coded or semi non-coded receiving mode. As a result, the signal/noise ratio at L2 is, at best, 13 dB lower than the mode of fully coded receiving and the difference between L1 and L2 signal powers for commercial receivers may be significantly over 10 dB. So, the information on the L2 signal lock loss may be considered as some indirect evidence of the GPS signal during strong scintillations and an indirect parameter to reflect the scintillation level for all kinds of GPS receivers on the global scale (Afraimovich et al., 2002, 2003, 2009). Those data may be a useful supplement to the data obtained by a few specialized monitors of ionospheric scintillations in the L range (Kintner and Ledvina, 2005), especially at mid-latitudes.

At first, we determine the coordinates of the subionospheric point at an altitude h_{max} in the geographical coordinate system.

$$\begin{aligned}
\phi_p &= \arcsin(\sin\phi_E\cos\psi_P + \cos\phi_B\sin\psi_P\cos\alpha_S)\\
\ell_P &= \ell_B + \arcsin(\sin\psi_P\sin\alpha_S\sec\phi_P)\\
\psi_p &= \frac{\pi}{2} - \theta_S - \arcsin\left(\frac{R_Z}{R_Z+h_{\max}}\cos\theta_S\right)
\end{aligned} \tag{1}$$

R_z is the Earth radius; (ϕ_p, ℓ_p), (ϕ_B, ℓ_B) are the geographical coordinates (latitude and longitude) of the subionospheric point and the point of GPS site; α_S and θ_S are the azimuth and elevation LOS, respectively. Fig. 1 shows the scheme of the LOS angular scanning. The axes ***h, Y,*** and ***X*** are directed zenithward, southward (***Y***) and eastward (***X***), respectively. The ***LOS*** arrows indicate the direction $\vec{r}$ along the LOS and the magnetic field line direction $\vec{B}$; $\boldsymbol{\theta_s}$ and $\boldsymbol{\theta_B}$ are the elevations of vectors $\vec{r}$ and $\vec{B}$, respectively; γ is the angle between the vectors $\vec{B}$ and $\vec{r}$.

As a direction of the magnetic field line we chose the direction of the local magnetic field at the altitude of ionosphere maximum h_{max} = 300 km. This assumption is appropriate when the direction of the local magnetic field vector doesn't change with altitude (at least for altitudes where the electron density is significant and there are intensive irregularities causing the scattering of GPS signals and L1 and L2 slips). We calculated the magnetic field line direction at the altitude h_{max} over the subionospheric point S_i by using the International Geomagnetic Reference Field

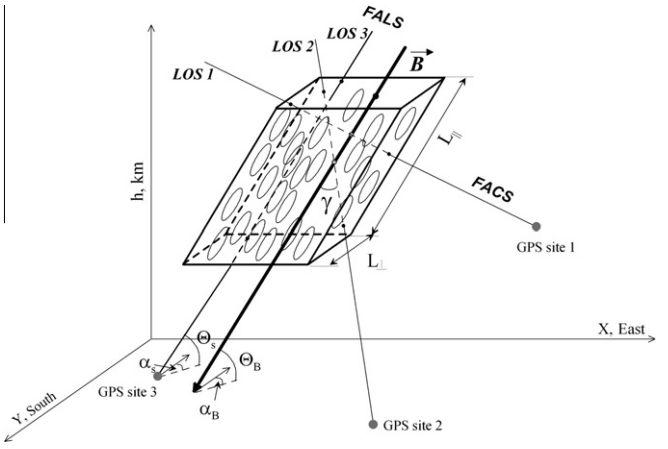

Fig. 1. The scheme of the LOS angular scanning. The axes ***h, Y,*** and ***X*** are directed zenithward, southward (***Y***) and eastward (***X***), respectively. The ***LOS*** arrows exhibit the direction $\vec{r}$ along LOS and the magnetic field line direction $\vec{B}$; α_S and α_B are the azimuth of vectors $\vec{r}$ and $\vec{B}$, respectively; θ_s and θ_B are the elevations of vectors $\vec{r}$ and $\vec{B}$, respectively; γ is the angle between the vectors $\vec{B}$ and $\vec{r}$. L_{II} и $L_{\perp}$ are the longitudinal and cross size of large scale bubble, elongated along the magnetic field line and containing the set of small scale irregularities. The LOS1 direction (magnetic normal) corresponds to the field of across scattering, FACS ($\gamma \sim 90°$) and LOS3 direction (magnetic zenith) is close to the field of aligned scattering, FALS ($\gamma \sim 0°$).

model IGRF-10 (<http://www.geomag.bgs.ac.uk/gifs/igrf_form.shtml>) and determine the angle γ between the vectors $\vec{r}$ and $\vec{B}$. Then, we calculate the histograms $N(\gamma)$ of L2 phase slips dependent on the angle γ value. The angular histogram bin $\Delta\gamma$ is equal to 1 degree for all our calculations.

For the adequate angular distribution calculation one should take into the real distribution of all LOS angular counts, or the background function ***S(γ)***. Function $S(\gamma)$ is equal to the total amount of 30-s samples for the chosen value of ***γ***. Normalized distribution ***P(γ)*** is a relative number of failures depending on a angle ***γ*** between the line-of-sight and the magnetic field direction.

$$P(\gamma) = N(\gamma)/S(\gamma) \quad (2)$$

Then we can analyze ***P(γ)*** and tried to find some angular (against magnetic field vector) features.

3. Experimental results

The L2 phase slip statistics on 12 Feb 2000 are shown in Fig. 2. Fig. 2a is the map of subionospheric points with L2 phase slips (11:00–14:00 UT, PRN 7, 20773 30-sec counts, black dots; PRN 13, 25474 counts, light grey dots; PRN16, 2758 counts, gray dots; and PRN24, 3175 counts, black gray dots). It has a good similarity with Fig. 3 in Ma and Marayama (2006). But here we can see the detailed distribution of L2 phase slips for selected PRNs. Fig. 2b shows the time dependence of L2 phase slip numbers $N(t)$ for the above satellite and the scale for PRN16 and PRN24 is shown on the right. The number of slips $N(t)$ increases abruptly (up to 230 receivers for PRN 13) in ten minutes. The total number of L2 phase slips is very significant. It corresponds to a very high level of scintillations, caused by GPS signal scattering on the intensive small scale irregularities.

The time interval 11:00–14:00 UT is further analyzed. The LOS trajectories of the sub-ionosphere points for the selected satellites (PRN07, PRN13, PRN16, PRN24) and GPS site 3054 (34.7°N, 137.7°E) are shown in Fig. 2c. The filled circle and filled gray area with black line stand for the LOS angular field near FALS and FACS, respectively, with angular window of about 10°, and black line in the gray area corresponds to $\gamma = 90°$. PRN07 and PRN13 move next to the magnetic zenith region and PRN16 and PRN 24 move next to the magnetic normal region. The thickened curves correspond to 11:00–14:00 UT, the filled circle and filled gray area with black line stand for the LOS angular field close to the FALS and the FACS, respectively, with angular window of about 10° and the thick black line in the gray area corresponds to $\gamma = 90°$. Fig. 2d presents the ***γ***-dependent normalized phase slip distribution ***P(γ)*** for corresponding satellites. The total number of L2 phase slips is indicated earlier. One can see that the L2 phase slips are registered close to the FALS (PRN 7 and PRN 13) and the FACS (PRN 16 and PRN 24).

In addition, the bulk of slips (up to 33%) were also observed at PRN13. A large number of slips were registered also at PRN7 (15%). For these satellites, the direction of signal propagation coincided with the direction of the local magnetic field vector. At the same time, the number of slips for the other pair of satellites is much lower. It is ~3% for PRN16 and 6% for PRN24. We propose to designate the first field of angular distribution as a field of aligned scattering and the other field as a field of across scattering. In Fig. 1 the LOS1 direction corresponds to the field of across scattering, FACS ($\gamma \sim 90°$) and the LOS3 direction is close to the field of aligned scattering, FALS ($\gamma \sim 0°$).

Fig. 2e shows the angular trajectories of the sub-ionosphere points for GEONET GPS site 3054 (34.7°N, 137.7°E) during entire 12 Feb 2000. Fig. 2f (black line) gives the total histograms of the background function $S(\gamma)$ for all PRN during entire 12 Feb 2000 ($\Sigma N = 17961082$). The light gray and dark gray lines are the initial series ***N(γ)*** of phase slips numbers and the normalized distribution ***P(γ)***, respectively. The total number of L2 phase slips is very significant ($\Sigma N = 149948$). The most probable value of $S(\gamma)$ corresponds to ~64° and the most probable values $P(\gamma)$ and $N(\gamma)$ corresponds to the FALS. One can see that the normalized distribution ***P(γ)*** differs from the initial series ***N(γ)*** significantly. The most probable value of γ for all L2 phase slips during entire 12 Feb 2000 is close to the FALS. Besides, there is increasing of slip numbers for angles γ near 90°. Similar angular dependencies were found for other time intervals (05:00–09:00 UT and 16:00–21:00 UT).

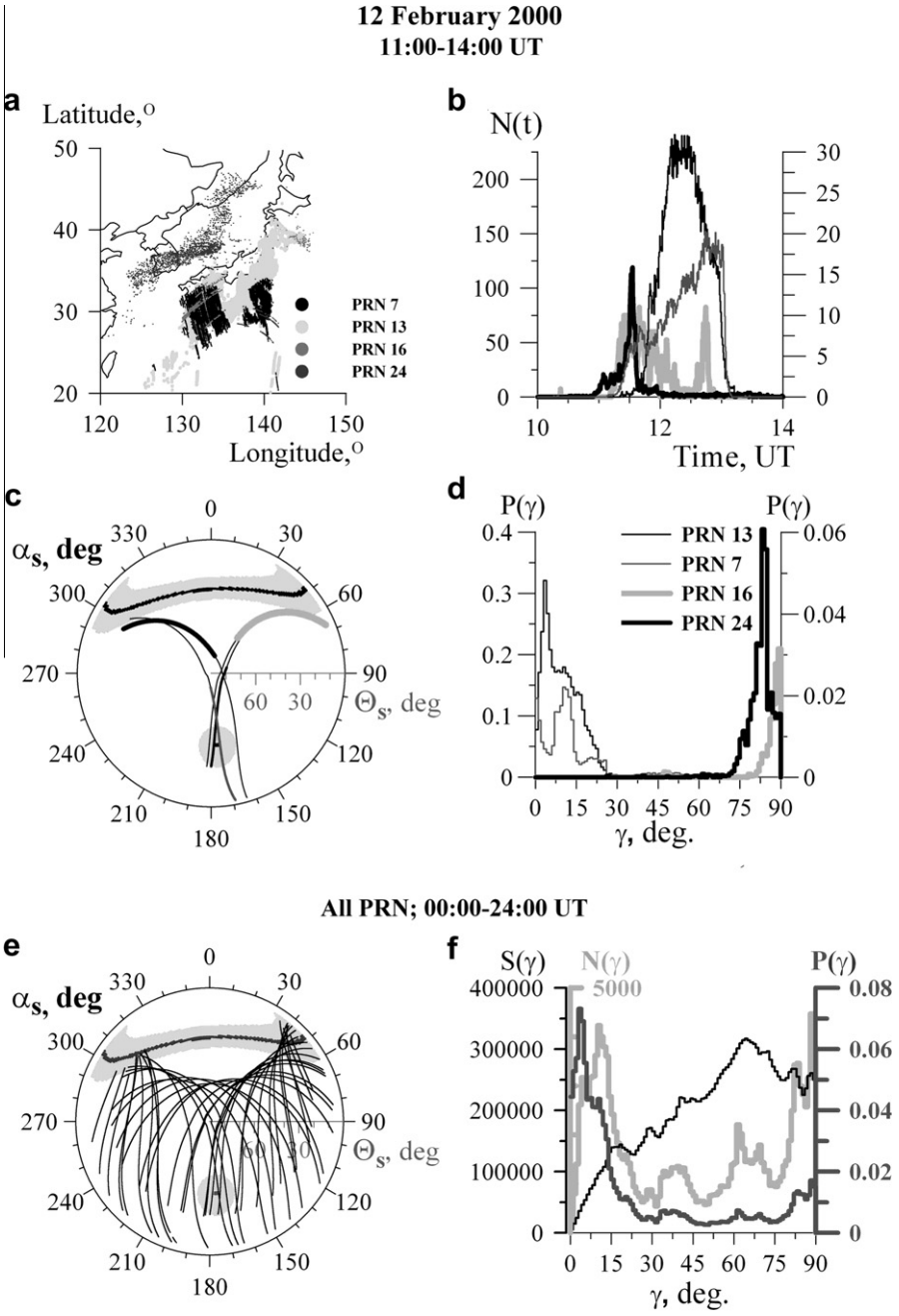

Fig. 2. The statistics of the L2 phase slips on 12 Feb 2000 (11:00–14:00 UT, PRN 7, 20773 counts, black dots; PRN 13, 25474 counts, light gray dots; PRN16, 2758 counts, grey dots; and PRN24, 3175 counts, dark grey dots): a) is the map of subionospheric points with the L2 phase slips; b) is the time dependence on the L2 phase slip numbers $N(t)$; the scale for PRN16 and PRN24 is shown on the right; c) are the trajectories of subionosphere points for GEONET GPS site number 3054 (34.7°N, 137.7°E); the filled circle and filled gray area with black line mark the LOS angular field of aligned scattering, FALS, and the field of across scattering, FACS, respectively, with angular window of about 10°; the black line in the gray area corresponds to $\gamma = 90°$. d) is the normalized phase slip distribution $P(\gamma)$ of angle γ between the direction $\vec{r}$ along the LOS and the magnetic field line direction $\vec{B}$; the thickened curves correspond to 11:00–14:00 UT; e and f are the same as c and d, but for all the PRN during entire 12 Feb 2000. Panel f presents the procedure of normalizing distribution $N(\gamma)$: the light grey, black and dark grey lines are the initial series $N(\gamma)$, the background function $S(\gamma)$, and the normalized distribution $P(\gamma) = N(\gamma)/S(\gamma)$, respectively.

4. Discussion and conclusions

GPS is used to detect mid-latitude field-aligned irregularities by line-of-sight angular scanning relative to the local magnetic field vector. It has shown that the total GPS L2 phase slips caused by FAIs over Japan during the recovery phase of the 12 Feb 2000 geomagnetic storm (Ma and Maruyama, 2006) corresponds to both the line-of-sight aligned to the magnetic field line and across the magnetic field line. At values of angles γ between 0° and 90° the effects of bubbles are less significant. One may see that values of slips density P sharply decrease. Nevertheless

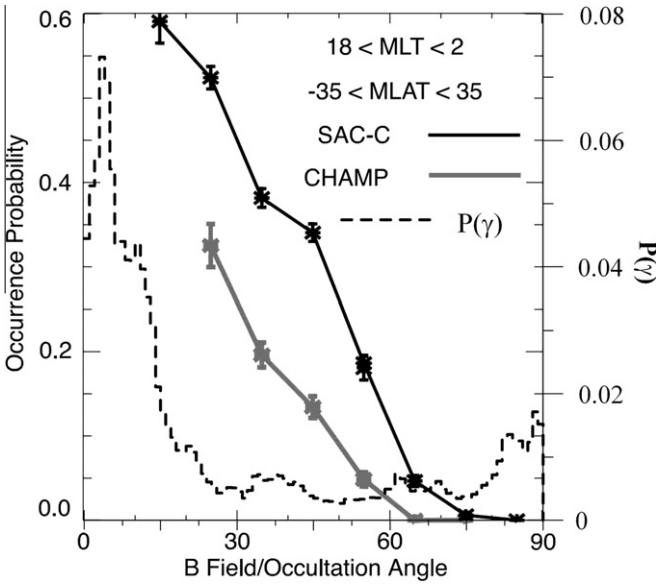

Fig. 3. Comparison between our normalized distribution $\boldsymbol{P(\gamma)}$ obtained from GEONET data, with the occurrence frequency for occultations with maximum S4 greater than 0.09 versus the angle between the occultation ray path and the magnetic field from CHAMP measurements (from Anderson and Straus, 2005).

these values don't equal a zero. Fig. 1 presents the simple scheme of the across and aligned scattering of GPS signal. Here L_{II} и $L_{\perp}$ are the longitudinal and cross size of a large scale bubble, elongated along the magnetic field line and containing the set of small scale irregularities. The LOS1 direction corresponds to the field of across scattering (magnetic normal), FACS ($\gamma \sim 90°$) and LOS3 direction is close to the field of aligned scattering (magnetic zenith), FALS ($\gamma \sim 0°$). Our results are in good agreement with the data on investigation of magnetic field orientation control of GPS occultation observations of equatorial scintillation during the LEO CHAMP, SAC-C and PICOSat detailed measurements by Anderson and Strauss (2005). The inclination of LEO orbits allowed studying the magnetic field dependence of scintillation index S4 on the magnetic field vector direction in a wide range of angles between the occultation ray path and the magnetic field.

Fig. 3 presents the comparison of our normalized distribution $\boldsymbol{P(\gamma)}$ of angle γ between the direction $\vec{r}$ along LOS and the magnetic field line direction $\vec{B}$ obtained from GEONET data, with the occurrence frequency for occultations with maximum S4 greater than 0.09 versus the angle between the occultation ray path and the magnetic field from CHAMP and SAC-C measurements (Anderson and Straus, 2005). SAC-C has the largest number of occultations and greatest probability of occurrence as it orbits has a half time within the post-sunset MLT sector where equatorial scintillations are most likely to occur. CHAMP has the smallest value of such measurements as it has a lower orbit altitude and, consequently, the smaller Fresnel scale. Despite these differences, the data from all the three satellites exhibit distinctly a strong dependence of the equatorial scintillation occurrence on the angle between the occultation ray path and the magnetic field. One can see that the S4 > 0.09 maximum occurrence probability and the normalized distribution $\boldsymbol{P(\gamma)}$ correspond to the small values of the angle between the occultation ray and the magnetic field.

We agree to the clear explanation by Anderson and Straus (2005) for similar dependence of the scintillation occurrence on the angle between the occultation ray path and the magnetic field (angle γ in our case). "We must examine the structure of ionospheric bubbles and the instabilities associated with them that lead to scintillation. Bubbles are formed in the bottomside F region and drift upwards under the influence of horizontal electric fields. The plasma drifts in the post sunset hours are faster near the F peak than at other altitudes, leading to a "C shape" when viewed with imagers from the ground (Woodman and LaHoz, 1976), or from high altitude (Kelley et al., 2003). However, when viewed at a single altitude, the bubbles are nominally stretched out in latitude, or along magnetic field lines (McClure et al., 1977). So the walls of the bubbles are extended vertically upward and stretched in the north-south direction along the magnetic field lines (see Fig. 1). Ionospheric interchange instabilities responding to the steep density gradient on the walls of the bubble in the F region produce the electron density irregularities responsible for radiowave scintillation. An occultation with a ray path of perpendicular to the magnetic field cuts across the bubbles perpendicular to the two walls of the bubble and passes through the regions of density irregularities on the walls only briefly (see Fig. 1). However, an occultation with a ray path of parallel to the magnetic field may pass along the edge of a bubble and the bubble wall, thus experiencing a path that may remain within the region of density irregularities for a significantly longer period than for occultations with ray path of perpendicular to the magnetic field. Put another way, the "slab thickness" of the irregularity region encountered by the GPS signals is larger when the ray path is aligned more closely to the direction of elongation of the bubble regions. Since scintillation strength increases with irregularity slab thickness (Yeh and Liu, 1982), the observed increase in scintillation occurrence for field-aligned conditions is reasonable".

The scattering in the field of aligned scattering, was studied well in numerous theoretical investigations and registered earlier repeatedly at equatorial (Kintner et al., 2004) and high (Wernik et al., 1990; Maurits et al., 2008) latitudes. Our results confirm the main conclusion of these investigations about the control over scintillation by the magnetic field direction. We check the investigations by Anderson and Straus (2005) where they, during radio occultation observations, revealed that scintillations increase when the angle between the ray/LOS and the magnetic field increases. However, the scintillation behavior is determined not only by the angle between the field and the ray/LOS (off-B angle; Wernik et al., 1990), but also by some other factors, such as the elevation angle, the irregularity morphology, etc.

The effect of GPS signal multipath propagation may be the alternative reason for such a deep radio-signal decay which causes the L2 signal lock at small angles γ. This results in emergence of scintillations at large angles between the propagation and the magnetic field (see Fig. 3) which is in good agreement with the observational data presented by Maurits et al. 2008. Possible explanation of the observed effect at $\gamma \sim 90°$ is as follows. When a NS signal crosses for a short time an irregularity, there may occur a large electron density time gradient due to their large mutual velocity. This can cause a greater velocity and acceleration of changes in the carrier phase and its loss of signal lock in the navigation receiver's coherent filtration loop.

It should be noted that the location of GPS receiver against the bubble is also important. At least at the ionospheric altitude a bubble should be placed next to the stations. Because of the extension range of the bubbles, the effects of the irregularities on GPS signal and hence the occurrence of phase slip should be different when GPS receivers' locations are different. Nevertheless the general dependence (increasing of slips probability for $\gamma = 0°$ and 90°) should be similar. Analyzing features of γ dependence on the dense GPS network you can conclude about the bubble presence.

The basic difference of our approach in investigating scintillations is using a rather substantial database of the malfunctions in denser GPS network. As it follows from the above comparison with the direct measurements of scintillations, such an indirect approach with using a close association of scintillations with GPS malfunctions provides a possibility to monitor scintillations and scintillation-related FAI with an accuracy enough sufficient. The effect of powerful HF radiation on the ionosphere has been investigated by using signals from high-orbiting GPS/GLONASS satellites (Tereshchenko et al., 2008). They revealed a quasi-stationary effect of magnetic zenith which leads to a decrease in the electron content and formation of electron density irregularities extended along the magnetic field lines. Those authors exhibited the efficiency of GPS/GLONASS satellite signal application to investigate the ionosphere affected by HF radiation. But it is very important to compare the above results with the statistics of the background TEC variation and scattering of GPS signals caused by natural field-aligned disturbances.

The scattering peculiarities of a transionospheric signal (when propagating along the magnetic field line) are necessary to be taken into account in all radio occultation experiments where inhomogeneous media in the ionosphere (Anderson and Straus, 2005), solar corona (Hewish and Symons, 1969; Pätzold et al., 1995), planets (Zhuk, 1980) and interstellar medium are investigated (Manchester and Taylor, 1977). Our results are important for ionospheric irregularity physics evolution and transionosphere radio wave propagation modeling. It is especially important during the coming solar maximum which will produce strong ionospheric storms and increase the background ionization level and level of ionosphere plasma irregularities (Kintner et al., 2009). Spatial-temporal features and modeling of mid-latitude FAIs will be further investigated in the near future.

Acknowledgements

We thank the referees who have enabled us to improve the manuscript through their valuable suggestions. The authors thank Prof. Potekhin A.P. and Dr. Medvedev A.V. for their interest in this work. We acknowledge the Geographical Survey Institute of Japan for providing us with GEONET data. The work was supported by Irkutsk State University individual Research Grant 111-02-000/8-03, the RFBR Grant 10-05-00113, the RF President Grant МК-3094.2010.5, the National Natural Science Foundation of China (NSFC) (Grant No.11043008), and the key program of Chinese Academy of Sciences (Grant No. KJCX2-YW-T26).

References

Afraimovich, E.L., Lesyuta, O.S., Ushakov, I.I., Voeykov, S.V. Geomagnetic storms and the occurrence of phase slips in the reception of GPS signals. Annals of Geophys. 45 (1), 55–71, 2002.

Afraimovich, E.L., Demyanov, V.V., Kondakova, T.N. Degradation of performance of the navigation GPS system in geomagnetically disturbed conditions. GPS Solut. 7 (2), 109–119, 2003.

Afraimovich, E.L., Astafieva, E.I., Demyanov, V.V., Gamayunov, I.F. Mid-Latitude Amplitude Scintillation of GPS Signals and GPS Performance Slips. Adv. Space Res. 43, 964–972, 2009.

Anderson, P.C., Straus, P.R. Magnetic field orientation control of GPS occultation observations of equatorial scintillation. Geophys. Res. Lett. 32, L21107, doi:10.1029/2005GL023781, 2005.

Astafyeva, E.I., Afraimovich, E.L., Voeykov, S.V. Generation of secondary waves due to intensive large-scale AGW traveling. Adv. Space Res. 41, 1459–1462, 2008.

Burke, W.J., Donatelli, D.E., Sagalyn, R.C., Kelley, M.C. Low density regions observed at high altitudes and their connection with equatorial spread F. Planet. Space Sci. 27, 593–601, 1979.

Conker, R.S., El-Arini, M.B., Hegarty, C.J., Hsiao, T. Modeling the effects of ionospheric scintillation on GPS/satellite-based augmentation system availability. Radio Sci. 38 (1), 1001, doi:10.1029/2000RS002604, 2003.

Cerruti, A.P., Ledvina, B.M., Kintner, P.M. Scattering height estimation using scintillating wide area augmentation system/satellite based augmentation system and GPS satellite signals. Radio Science 41, RS6S26, doi:10.1029/2005RS003405, 2006.

Gurtner, W. The Receiver Independent Exchange Format Version 2. 1993. Available from: <http://igscb.jpl.nasa.gov/igscb/data/format/rinex2.txt>.

Hewish, A., Symons, M.D. Radio investigation of the solar plasma. Planet. Space Science 17 (3), 313–320, 1969.

Huang, C.-S., Foster, J.C., Sahai, Y. Significant depletions of the ionospheric plasma density at middle latitudes: A possible signature of equatorial spread F bubbles near the plasmapause. J. Geophys. Res. 112, A05315, 2007.

Interface Control Document: ICD-200c. Available from: <http://www.navcen.uscg.mil/pubs/gps/icd200/S>.

Jin, S.G., Luo, O., Park, P. GPS observations of the ionospheric F2-layer behavior during the 20th November 2003 geomagnetic storm over South Korea. J. Geod. 82 (12), 883–892, doi: 10.1007/s00190-008-0217-x, 2008.

Kelley, M.C., Makela, J.J., Paxton, L.J., Kamalabadi, F., Comberiate, J.M., Kil, H. The first coordinated ground- and space-based optical observations of equatorial plasma bubbles. Geophys. Res. Lett. 30 (14), 1766–1769, doi:10.1029/2003GL017301, 2003.

Kintner, P.M., Ledvina, B.M., de Paula, E.R., Kantor, I.J. Size, shape, orientation, speed, and duration of GPS equatorial anomaly scintillations. Radio Sci. 39 , RS2012, doi:10.1029/2003RS002878, 2004.

Kintner, P.M., Humphreys, T., Hinks, J. GNSS and ionospheric scintillation. How to Survive the Next Solar Maximum. Inside GNSS 4 (4), 22–31, 2009.

Kintner, P.M., Ledvina, B.M. The ionosphere, radio navigation, and global navigation satellite systems. Adv. Space Res. 35 (5), 788–811, 2005.

Ledvina, B.M., Makela, J.J., Kintner, P.M. First observations of intense GPS L1 amplitude scintillations at midlatitude. Geophys. Res. Lett. 29 (14), 10.1029/2002GL014770, 2002.

Ledvina, B.M., Kintner, P.M., Makela, J.J. Temporal properties of intense GPS LI amplitude scintillations at midlatitudes. Radio Sci. 39, RS1S18, doi:10.1029/2002RS002832, 2004.

Ledvina, B.M., Makela, J.J. First observations of SBAS/ WAAS scintillations: Using collocated scintillation measurements and all-sky images to study equatorial plasma bubbles. Geophys. Res. Lett. 32, L14101, doi:10.1029/2004GL021954, 2005.

Ma, G., Maruyama, T. A super bubble detected by dense GPS network at east Asian longitudes. Geophys. Res. Lett. 33, L21103, doi: 10.1029/2006GL027512, 2006.

Manchester, R.N., Taylor, J.H. Pulsars. Freeman, San Francisco, p. 176, 1977.

Maurits, S.A., Gherm, V.E., Zernov, N.N., Strangeways, H.J. Modeling of scintillation effects on high-latitude transionospheric paths using ionospheric model (UAF EPPIM) for background electron density specifications. Radio Sci. 43, RS4001, doi:10.1029/2006RS003539, 2008.

McClure, J.P., Hanson, W.B., Hoffman, J.H. Plasma bubbles and irregularities in the equatorial ionosphere. J. Geophys. Res. 82, 2650–2656, 1977.

Meggs, R.W., Cathryn, N.M., Smith, A.M. An investigation into the relationship between ionospheric scintillation and loss of lock in GNSS receivers. Proceedings of the Meeting RTO-MP-IST-056 Characterising the Ionospere. Paper 5. Alaska, Fairbanks, US, June 12–16, 2006.

Pätzold, M., Neubauer, F.M., Bird, M.K. Radio occultation studies with Solar Corona Sounders. Space Science Reviews, 77–80, 1995.

Perov, A.I., Kharisov, V.N. GLONASS: Principles of Construction and Functioning. Radiotekhnika, Moscow, 2005, 720 (in Russian).

Skone, S.H. The impact of magnetic storms on GPS receiver performance. Geodesy 75 (9–10), 457–468, doi:10.1007/ S001900100198, 2001.

Tereshchenko, E.D., Milichenko, A.N., Frolov, V.L., Yurik, R.Yu. An observation of the magnetic zenith effect by using GPS/GLONASS satellites signals. Radiophysics and Quantum Electronics 51 (11), 842–846, 2008.

Yeh, K.C., Liu, C.H. Radio wave scintillations in the ionosphere. Proc. IEEE 70 (4), 324–360, 1982.

Wernik, A.W., Liu, C.H., Franke, S.J., Gola, M. High-latitude irregularity spectra deduced from scintillation measurements. Radio Sci. 25 (5), 883–895, 1990.

Woodman, R.F., LaHoz, C. Radar observations of F region irregularities. J. Geophys. Res. 81, 5447–5466, 1976.

Zhuk, N. Scintillation studies of cosmic source angular structure (Review). Radiophysics and Quantum Electronics 23 (8), 597–615, doi: 10.1007/ BF01041203, 1980.